

A New Repulsive Type Magnetic Bearing: Modeling and Control

著者 (英)	Mukhopadhyay S.C., Ohji T., Iwahara Masayoshi, Yamada Sotoshi, Matsumura Fumio
journal or publication title	Proceedings of the International Conference on Power Electronics and Drive Systems
volume	1
page range	12-18
year	1997-05
URL	http://doi.org/10.24517/00048888

doi: 10.1109/PEDS.1997.618629

A New Repulsive Type Magnetic Bearing - Modeling and Control

S.C.Mukhopadhyay, T.Ohji, M.Iwahara, S.Yamada and F.Matsumura
Laboratory of Magnetic Field Control and Applications, Faculty of Engineering,
Kanazawa University, Kodatsuno 2-40-20, Kanazawa 920, Japan.

Abstract - This paper reports on the development of a new repulsive type magnetic bearing system whose radial bearing section makes good utilization of the repulsive forces between stator and rotor permanent magnets resulting a simplified axial control scheme. The shape and configuration of permanent magnet is the most critical component for satisfactory operation of this type of magnetic bearing. In this paper, modeling of the permanent magnets has been done with the help of finite element analysis and the nature of the repulsive forces and stiffnesses are estimated along the three directions. Using the forces and expressing the rotor dynamics the issue of modeling a real physical repulsive type magnetic bearing system is discussed. The controller has been configured around digital signal processor. A prototype model has been designed and fabricated in our laboratory and experiments are carried out.

Keywords : Repulsive type magnetic bearing, permanent magnet, finite element analysis, digital signal processor, modeling.

1. Introduction

Magnetic bearing consisting of permanent magnets and controlled electromagnets offer numerous advantages such as long life, extremely reliable, frictionless nature, lubrication free operation, low losses adjustable damping, and stiffness characteristics. These become indispensable the applications such as turbomolecular pump, space applications, vacuum and clean room atmosphere, fly wheel energy storage etc. Repulsive type magnetic bearing consisting of permanent magnets and controlled electromagnet have the advantages of less number of electromagnets and simplified control compared to active magnetic bearing. Many research papers have been published on magnetic bearings using permanent magnets [1]-[4]. But the satisfactory operation of this type magnetic bearing is strongly depended on the characteristics of the permanent magnet and its configuration in the bearing system. This paper reports on the development of a new repulsive type magnetic bearing system. It investigates the placement of permanent magnets for better stiffness and the digital signal processor based controller for the

overall stability for repulsive type magnetic bearing system whose radial bearing section makes good utilization of the repulsive force between stator and rotor permanent magnets. The configuration of permanent magnets analyzed by finite element approach helps in better stiffness eliminating the radial controllers by choosing the suitable arrangement of the permanent magnets. The axial control have been implemented by adjusting the currents of the electromagnets, the controller for which have been configured around a digital signal processor. A prototype model have been designed and fabricated in our laboratory and experiments are carried out.

The main work in this project can be summarized as

- (1) Finite element analysis of stator and rotor permanent magnets and determination of the magnitude and nature of the variation of repulsive forces with distance along three directions.
- (2) Expression of the forces by suitable numerical equations,
- (3) State space modeling of the bearing system,
- (4) Design of the controller,
- (5) Implementation of the controller around the digital signal processor,
- (6) Experiments on the system.

2. System Configuration

The structure of the repulsive type magnetic bearing system is shown schematically in Fig.1. The stator and rotor permanent magnets are placed at two sides and the electromagnets, rotor and stator of the motor are in the middle. Due to the repulsive forces between the stator and rotor permanent magnet, the rotor floats in that magnetic field but the system is an unstable one. The objective of the control is to held the rotor stably and firmly without any contact by controlling the attractive forces of the electromagnets. The system have been designed and fabricated in our laboratory. The stator permanent magnet is made of Nd-Fe-B magnet whereas the rotor permanent magnet is from Sr-Ferrite magnet. The total mass of the rotor is 8kg. The gap-sensor is used to measure the gap between the rotor and the electromagnet.

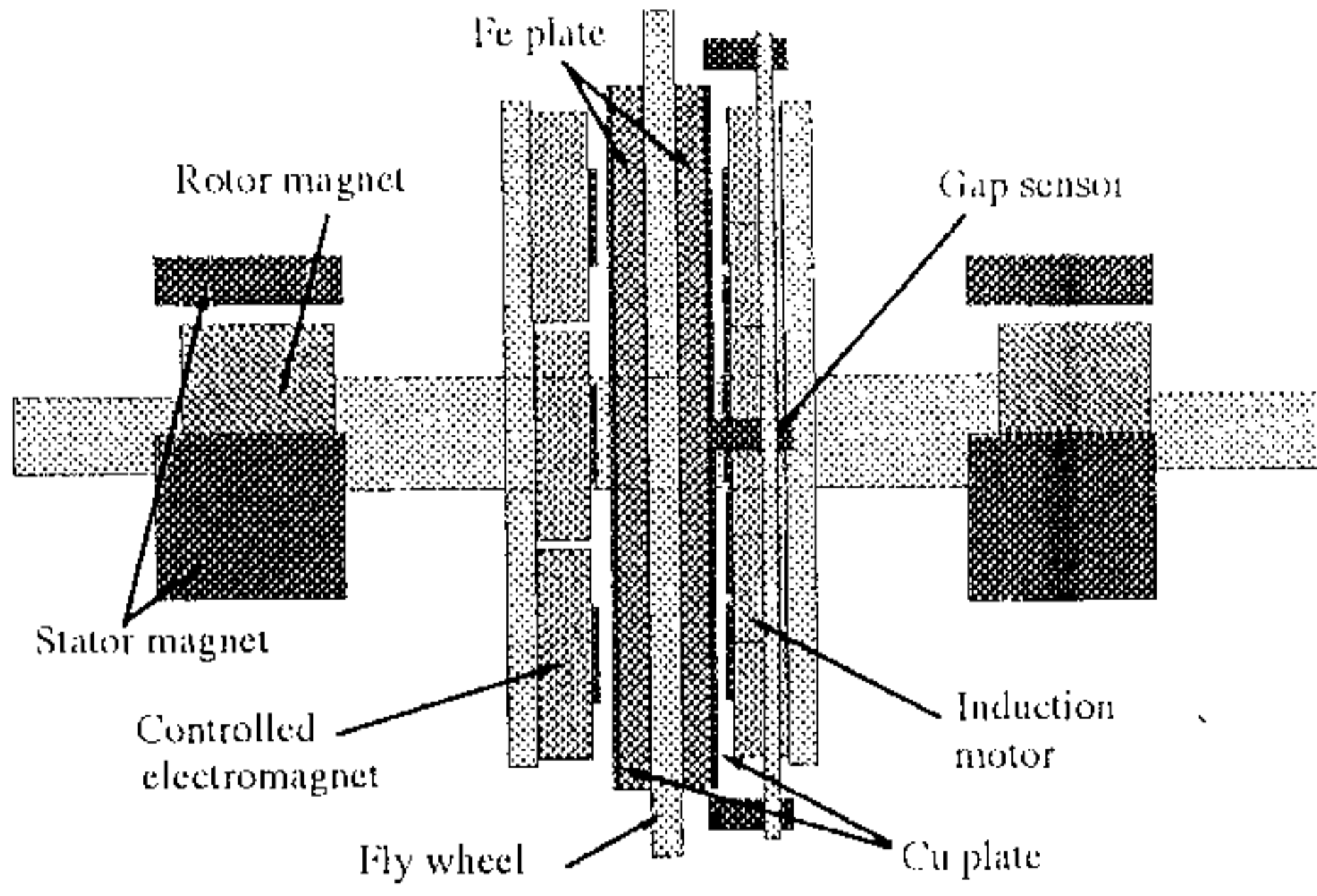


Fig. 1 Configuration of magnetic bearing system.

3. FE Analysis of PM Configuration

As the permanent magnet characteristics and its configuration in the system has a strong influence on the working of repulsive type permanent magnet bearing system, the knowledge of PM characteristics is essential. For developing the new type of magnetic bearing system the nature and magnitudes of the repulsive forces acting between the stator and rotor permanent magnets of the configuration shown in Fig.2 has been characterized by finite element method. By positioning the rotor magnets with respect to stator magnets, the forces along the three directions have been calculated.

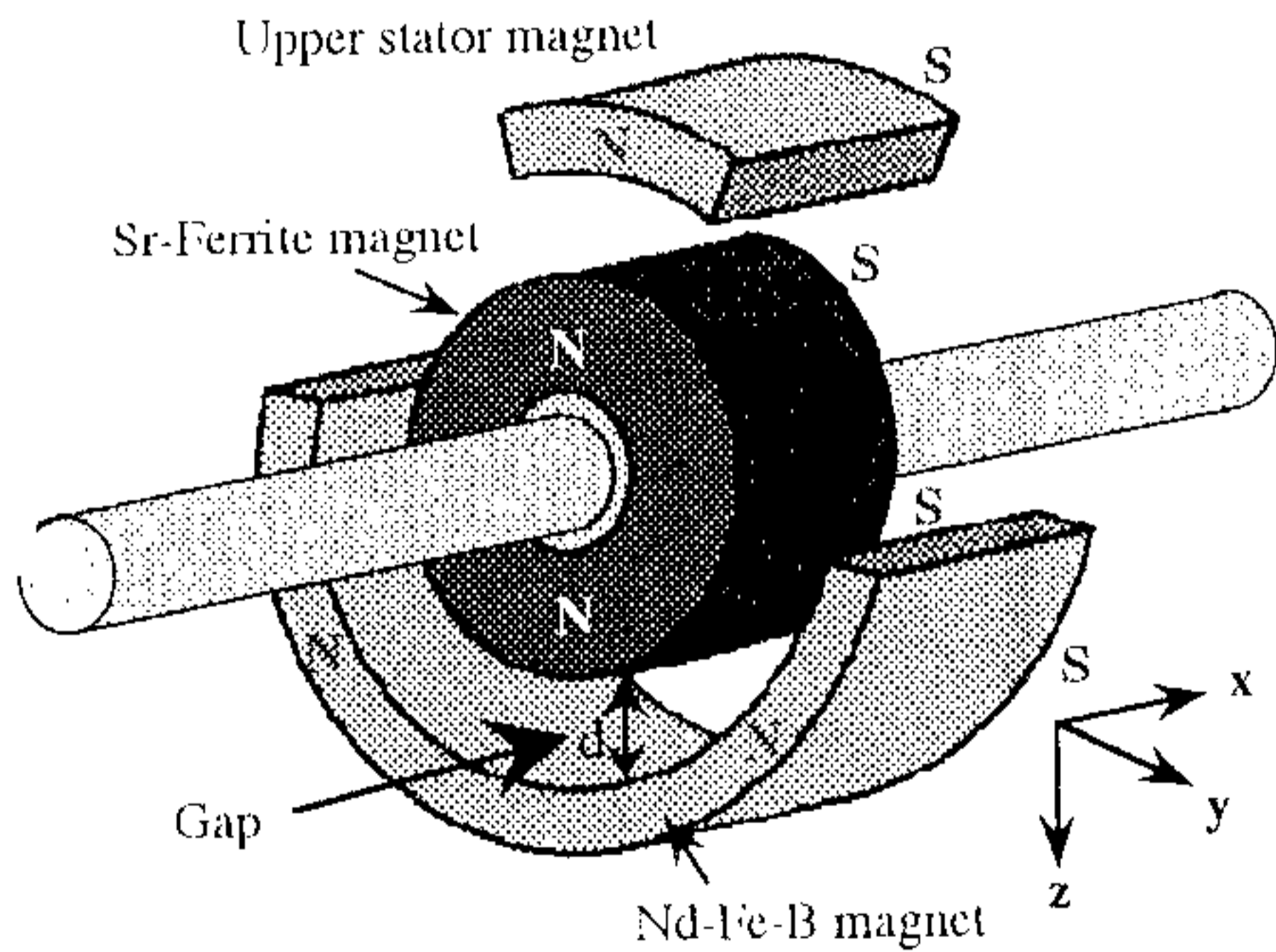


Fig. 2 Configuration of permanent magnets for bearing.

The variation of repulsive force along z-axis, f_z with the gap for different values of x are shown in Fig.3. The variation of f_x (force along x-axis) with x-axis distance and f_y (force along y-axis) with y-axis distance for different values of gap distance, d , are shown in Figs.4 and 5 respectively.

The repulsive forces acting between the stator and rotor permanent magnets has also been measured experimentally. The measured force characteristic along z-axis, f_z with the gap for different values of x are shown

in Fig.6. The measured characteristics of f_x with x-axis distance and f_y with y-axis distance for different values of d are shown in Figs.7 and 8 respectively. It is seen that the nature of the calculated characteristics from FEM almost matches the measured characteristics. Fig.9 shows the stiffness along the z-axis.

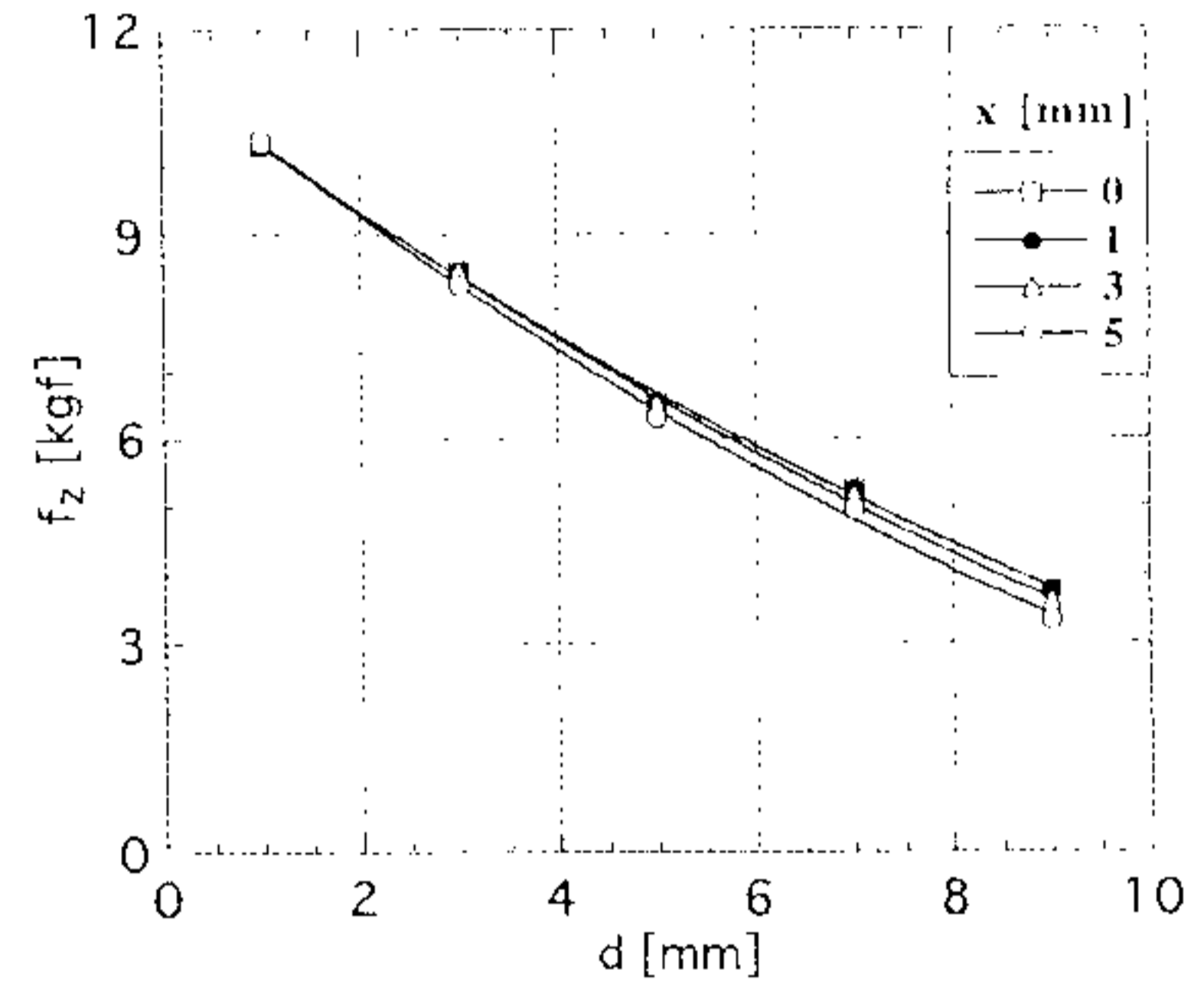


Fig.3 Calculated repulsive force along z-axis

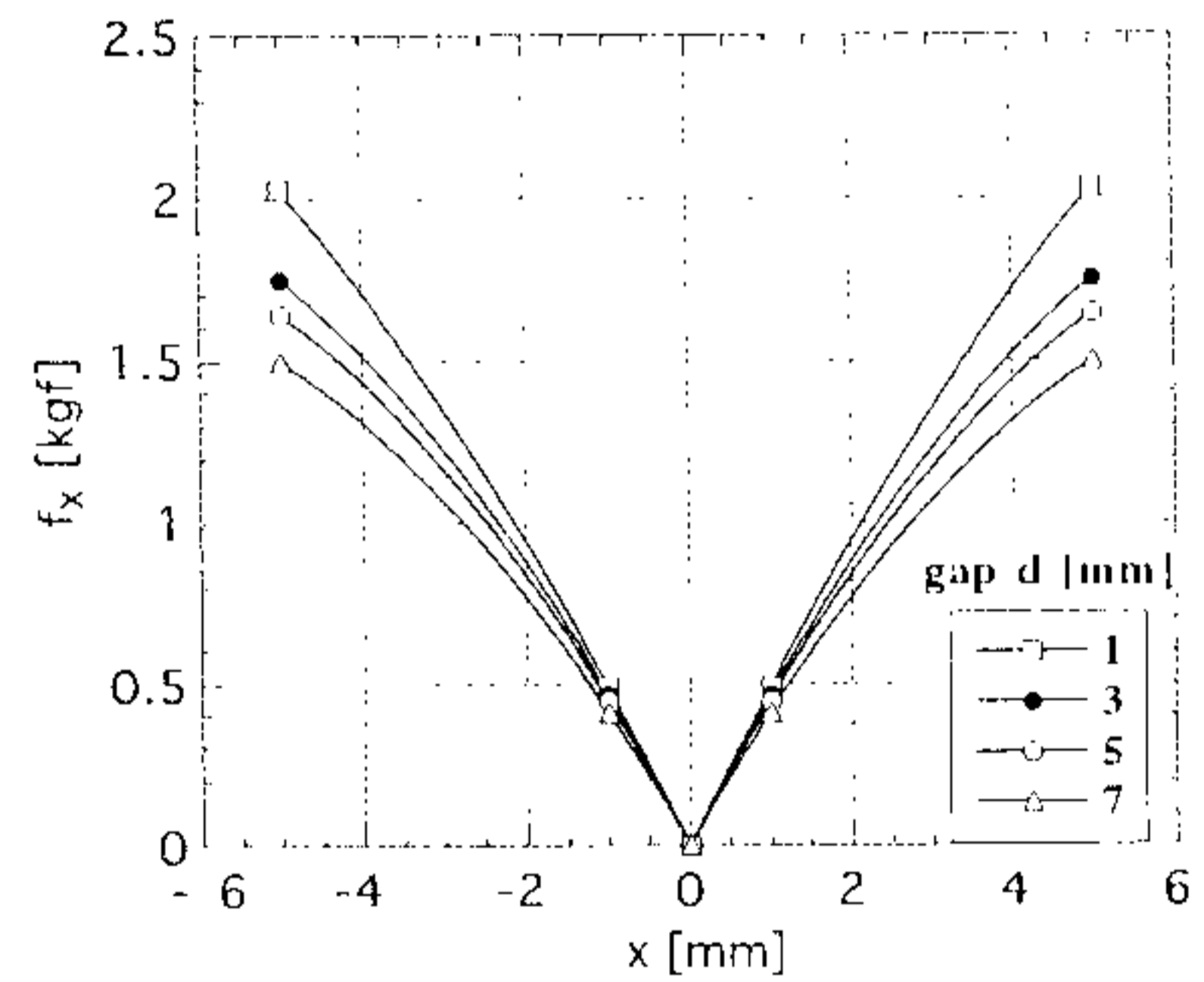


Fig.4 Calculated repulsive force along x-axis

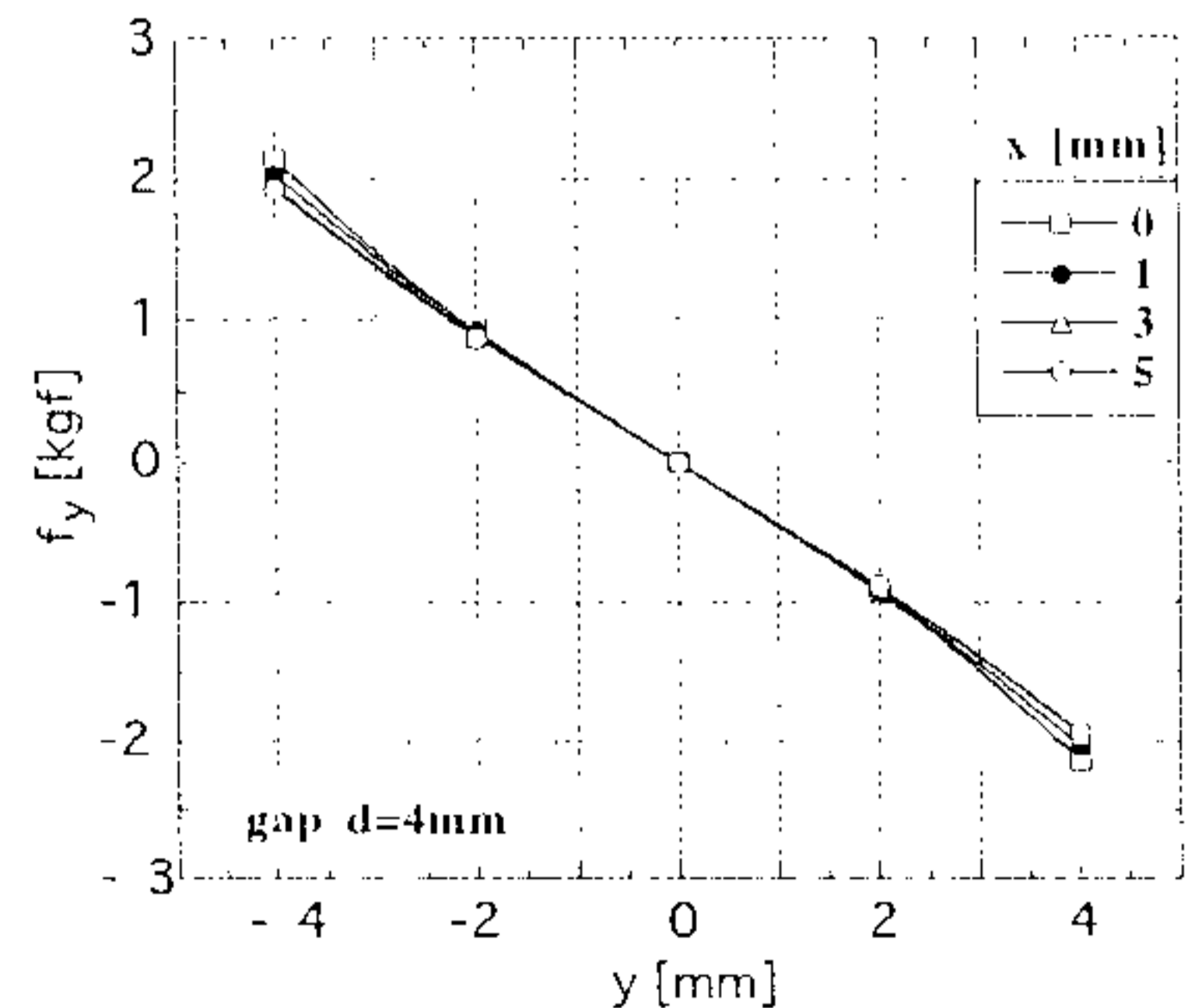


Fig. 5 Calculated repulsive force along y-axis.

4. Mathematical Representation of Forces

For the modeling of the bearing system the repulsive forces between the stator and rotor permanent magnet are expressed by approximate equations which represent the nature of the forces. The approximate equations are

Along x-axis The variation of the repulsive force acting along x-axis with x-axis distance is expressed as

$$f_c = S_c(g_c - A_x) + F_c \quad (c = lx, rx) \quad (1)$$

Along y-axis : The variation of the repulsive force acting along y-axis with y-axis distance is expressed as

$$f_b = -R_b g_b \quad (b = ly, ry) \quad (2)$$

Along z-axis : The variation of the repulsive force acting along z-axis with z-axis distance is expressed as

$$f_a = -Q_a(g_a - A_z) + F_a \quad (a = lz, rz) \quad (3)$$

where S_c , F_c , R_b , Q_a and F_a are different constants calculated from the measured characteristics at the operating point. The force-distance characteristics along z-axis is non-linear in nature. The linearized equations are used in the modeling of the system. The above equations represent the variations of the forces in particular axis while the positions along the other axes are constant. The force along one axis is also dependent though small and sometimes negligible, on the variations of other axis distances. Based on this idea the actual representation of the force along three axes is shown by Eq.(4).

$$\begin{bmatrix} f_c \\ f_b \\ f_a \end{bmatrix} = \begin{bmatrix} \partial f_c / \partial g_c & \partial f_c / \partial g_b & \partial f_c / \partial g_a \\ \partial f_b / \partial g_c & \partial f_b / \partial g_b & \partial f_b / \partial g_a \\ \partial f_a / \partial g_c & \partial f_a / \partial g_b & \partial f_a / \partial g_a \end{bmatrix} \begin{bmatrix} g_c \\ g_b \\ g_a \end{bmatrix} + \begin{bmatrix} \alpha \\ \beta \\ \gamma \end{bmatrix} \quad (4)$$

at operating point

The partial derivatives are calculated from the experimental characteristics at the normal equilibrium operating point.

5. Modeling of the System

During modeling of the rotor, a few assumptions are made like (1) rotor is a rigid body dynamics and (2) rotor maintains symmetry around the rotating axis. The forces acting on the rotor are shown in Fig.10. Here f_1, f_2, f_3 and f_4 are the forces acting on the rotor by four electromagnets, f_{lx}, f_{ly} , and f_{lz} are the forces on left sides due to permanent magnets and f_{rx}, f_{ry} and f_{rz} are corresponds to that of right side due to permanent magnets.

The basic dynamic equations[5]-[8] are listed below from Eqs.(5) to (10).

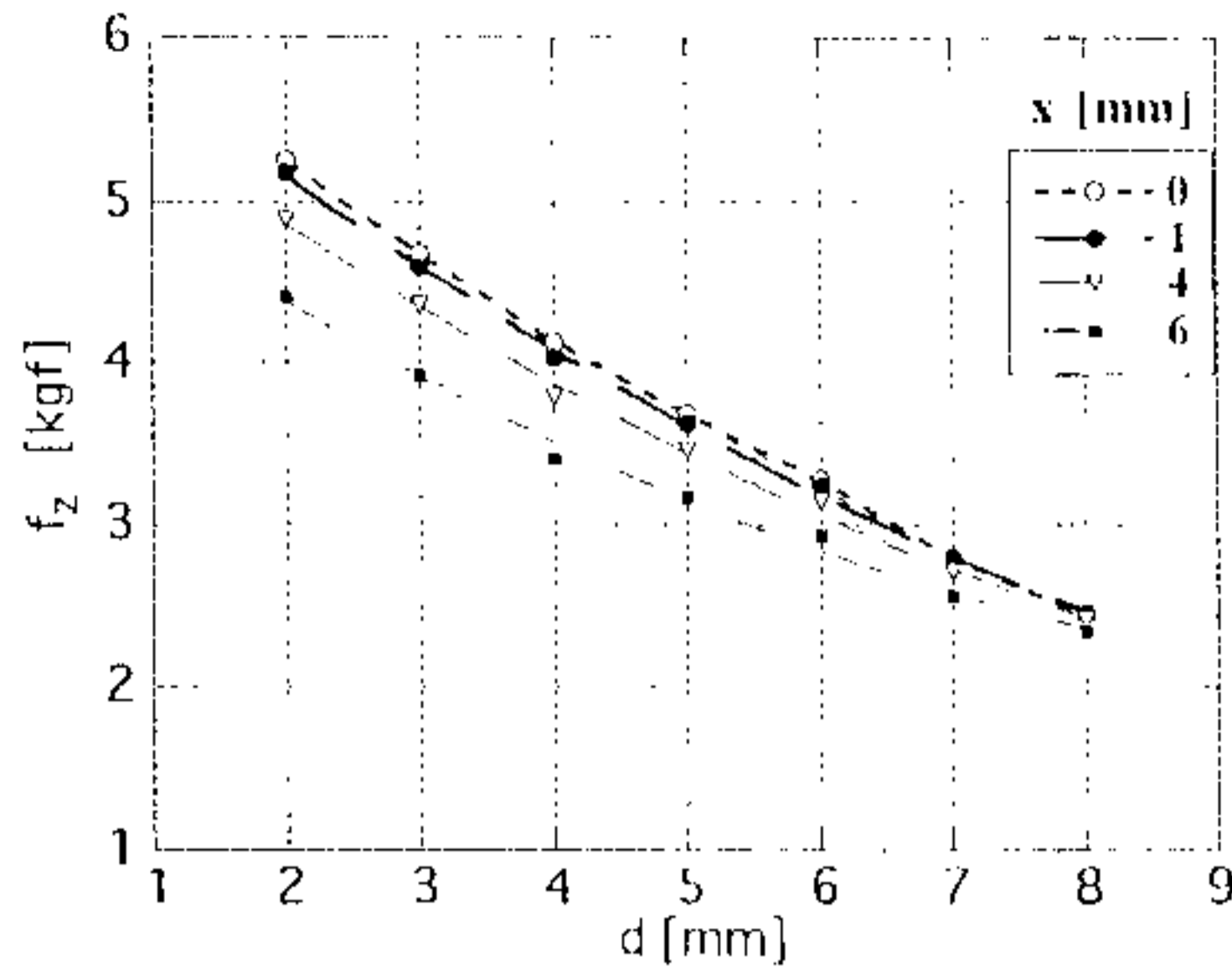


Fig.6 Variation of repulsive force with gap.

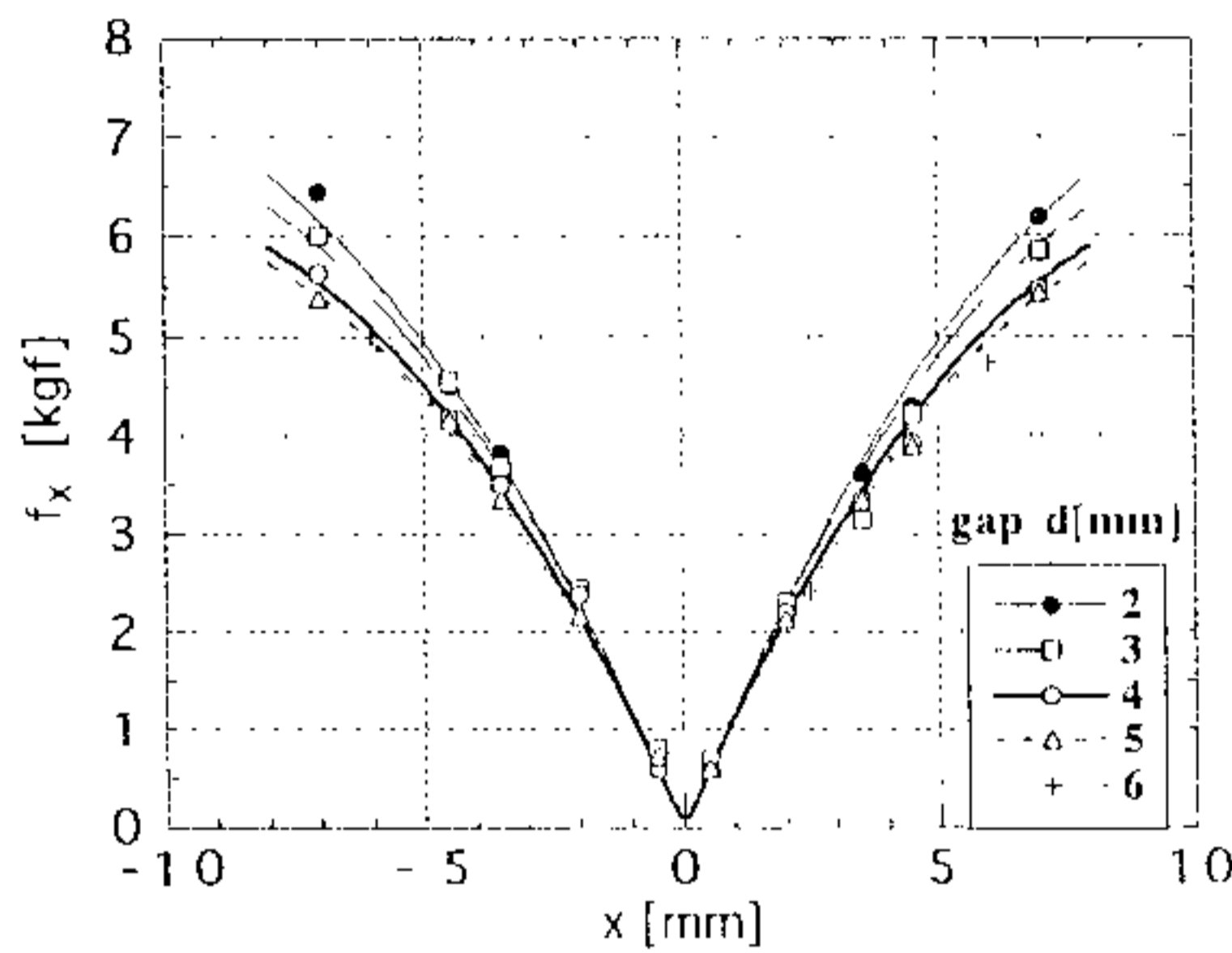


Fig.7 Variation of repulsive force with x-axis distance.

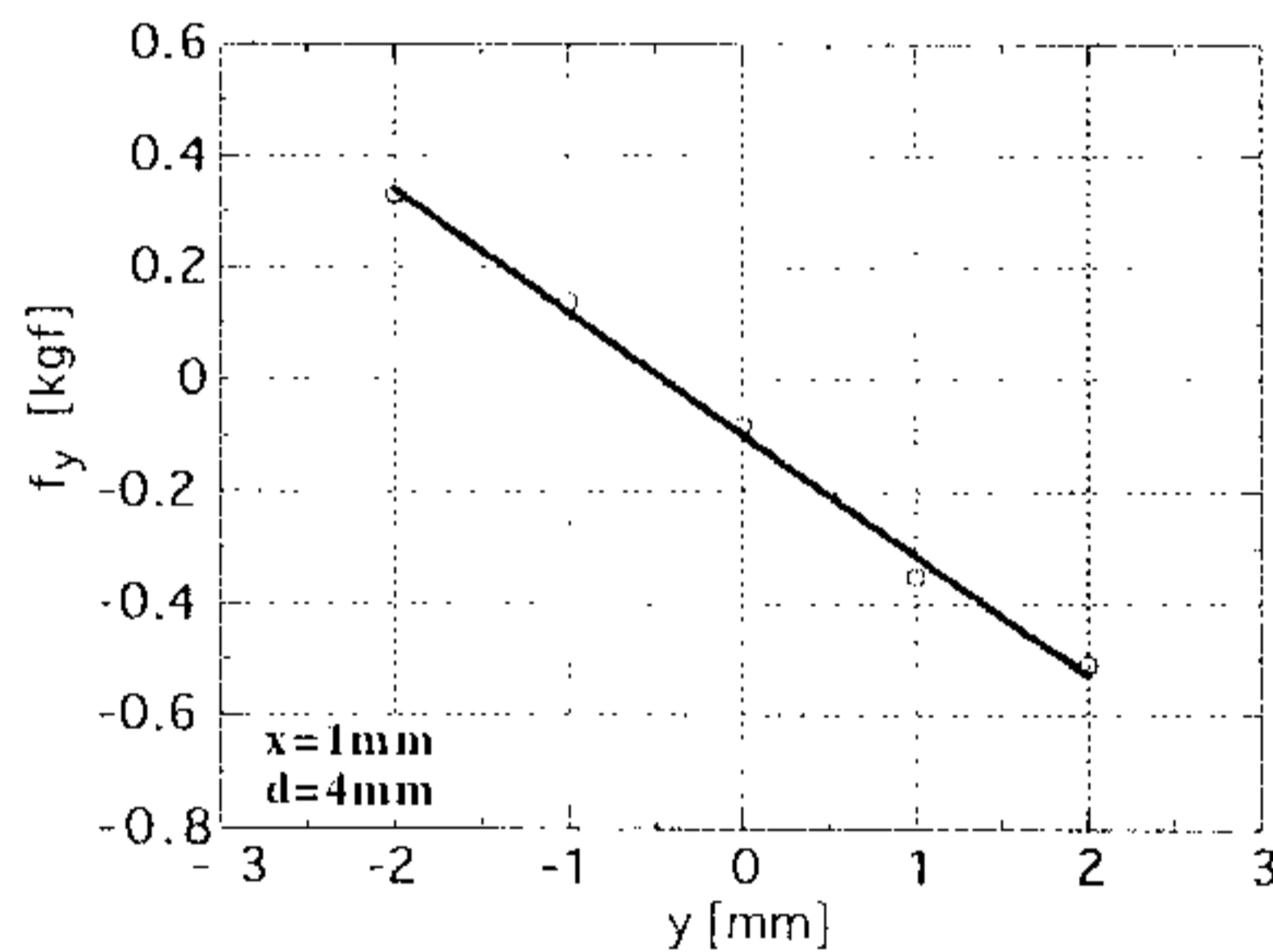


Fig.8 Variation of repulsive force with y-axis distance.

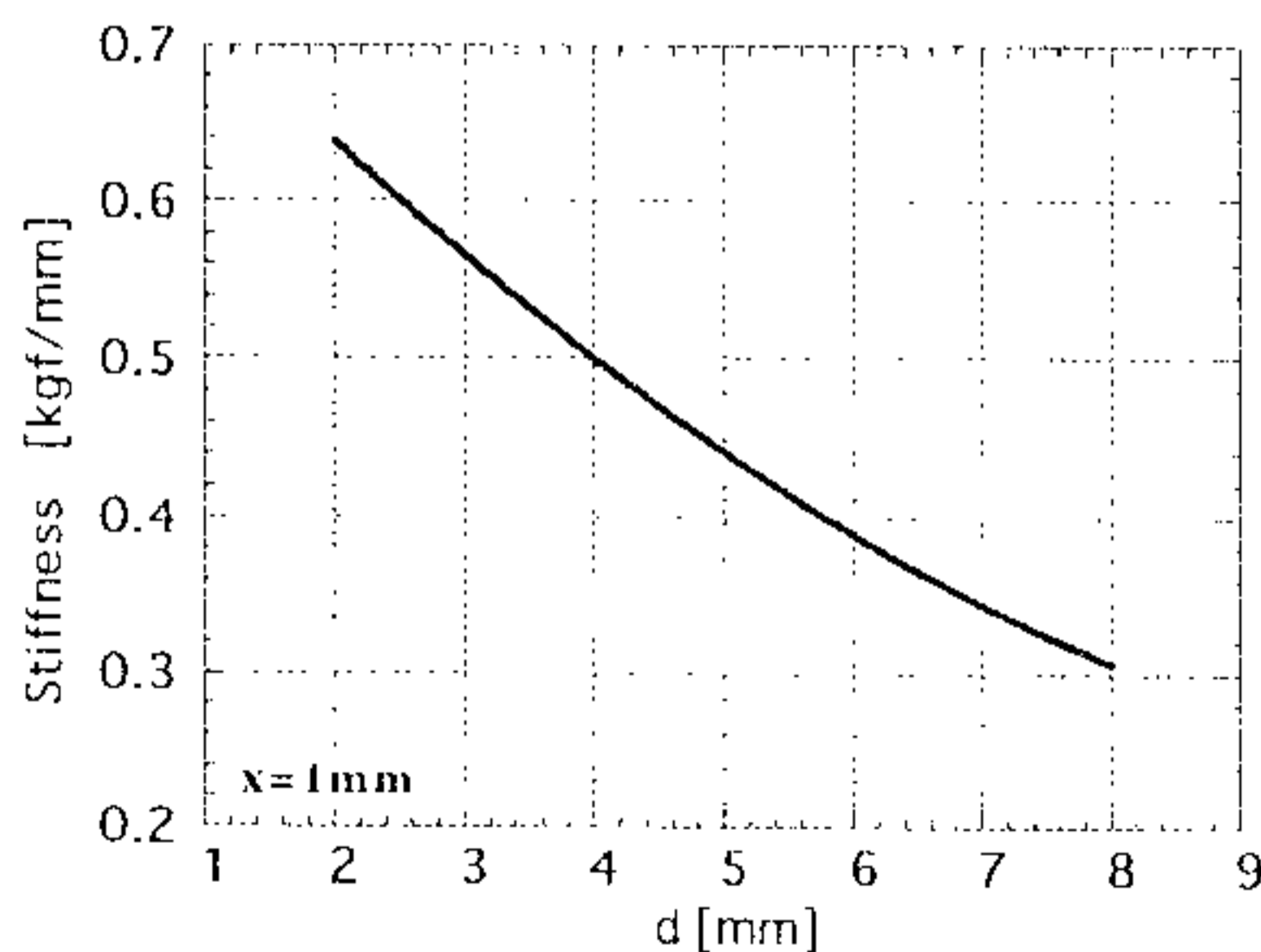


Fig.9 z-direction stiffness.

$$X = m(\dot{u} + qw - rv) \quad (5)$$

$$Y = m(\dot{v} + ru - pw) \quad (6)$$

$$Z = m(\dot{w} + pv - qu) \quad (7)$$

$$L = J_x \dot{p} \quad (8)$$

$$M = J_y \dot{q} + (J_x - J_y)rp \quad (9)$$

$$N = J_y \dot{r} - (J_x - J_y)pq \quad (10)$$

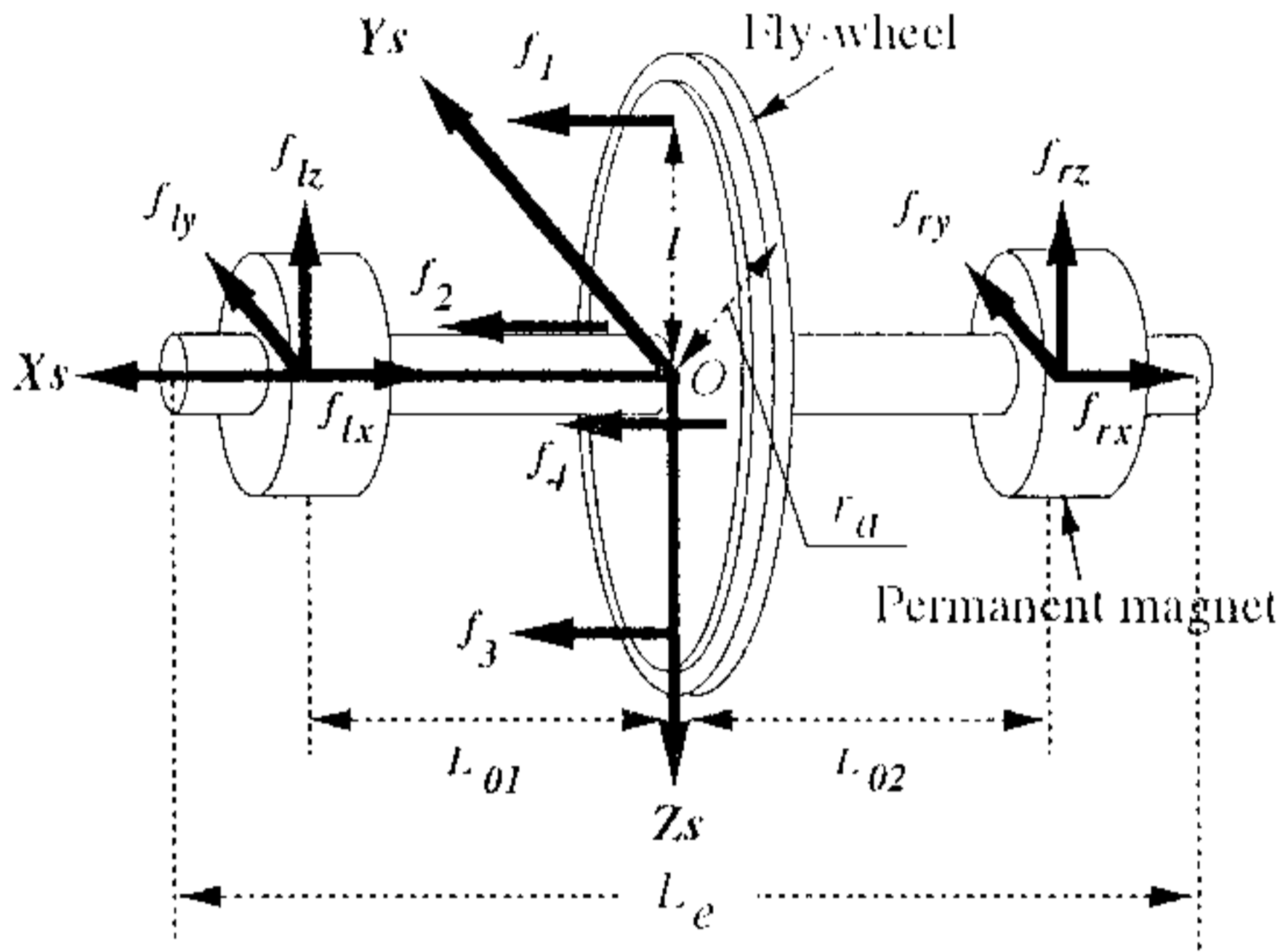


Fig.10 Modeling of rotor.

Where X , Y and Z are the scalar components of forces exerted on the rotor. L , M and N are the scalar components of moments about the mass center of the rotor. Angular velocity of roll, pitch and yaw are denoted by p , q and r respectively and the linear velocity components by u , v and w . ϕ , θ and ψ are the angle of roll, pitch and yaw respectively.

The forces acting on the rotor are :

Along x -axis

$$f_1 + f_2 + f_3 + f_4 - f_{tx} - f_{rx} \quad (11)$$

Along y -axis

$$f_{ty} + f_{ry} \quad (12)$$

Along z -axis

$$mg - f_{tz} - f_{rz} \quad (13)$$

The torques operating on the rotor are :

Around x -axis

$$T_m - p\rho - T_o \quad (14)$$

Around y -axis

$$f_{tx}L_{01} - f_{rx}L_{02} - f_1l + f_3l \quad (15)$$

Around z -axis

$$f_{ty}L_{01} - f_{ry}L_{02} - f_2l + f_4l \quad (16)$$

The airgaps are expressed as

$$g_1 = W_1 - x_s + l\theta, g_{1a} = A_1 - x_s, g_{1v} = y_s + L_{01}\psi,$$

$$g_2 = W_2 - x_s + l\psi, g_{2a} = A_1 - x_s, g_{2v} = y_s - L_{02}\psi,$$

$$g_3 = W_3 - x_s - l\theta, g_{3a} = A_2 - z_s + L_{01}\theta,$$

$$g_4 = W_4 - x_s - l\psi, g_{4a} = A_2 - z_s - L_{02}\theta \quad (17)$$

Based on the above discussions the basic state equations are given by Eqs.(18) to (22)

$$m\ddot{x}_s = f_1 + f_2 + f_3 + f_4 - f_{tx} - f_{rx} \quad (18)$$

$$m\ddot{y}_s = f_{ty} + f_{ry} \quad (19)$$

$$m\ddot{z}_s = mg - f_{tz} - f_{rz} \quad (20)$$

$$\ddot{\theta} = -\frac{pJ_x}{J_y}\dot{\psi} + \frac{L_{01}}{J_y}f_{tz} - \frac{L_{02}}{J_y}f_{rz} + \frac{l}{J_y}(f_3 - f_1) \quad (21)$$

$$\ddot{\psi} = \frac{pJ_x}{J_y}\dot{\theta} + \frac{L_{01}}{J_y}f_{ty} - \frac{L_{02}}{J_y}f_{ry} + \frac{l}{J_y}(f_4 - f_2) \quad (22)$$

For the formulation of the electromagnets the following assumptions are made.

- (1) The force produced by the electromagnet is proportional to the square of current and inversely proportional to the square of gap distance
- (2) All the electromagnets are of identical structure,
- (3) Deviation around the normal equilibrium operating point is small.

The equations of the electromagnets are written as

$$e_j = L\frac{di_j}{dt} + Ri_j \quad (23)$$

$$f_j = k\left(\frac{i_j}{g_j}\right)^2 \quad (24)$$

Linearizing the operating characteristics of the electromagnet around the normal equilibrium operating point, expressing them by the deviated quantities from the steady state values, we get

$$e'_j = L\frac{di'_j}{dt} + Ri'_j \quad (25)$$

$$f'_j = 2F_j\left(\frac{i'_j}{I_j} - \frac{g'_j}{W}\right) \quad (26)$$

Using equations Eqs.(18) to (22) and Eqs.(25)-(26), taking x_s , y_s , z_s , θ and ψ and their derivatives and the deviated currents of electromagnets i'_1 , i'_2 , i'_3 and i'_4 , the state space equations are obtained in matrix form as shown in Eq.(27). The signals of the gap-sensors are taken as output and the output equation is given by Eq.(28)

$$\frac{d}{dt} \begin{bmatrix} x_1 \\ z \\ i \end{bmatrix} = \begin{bmatrix} \mathbf{0} & \mathbf{I} & \mathbf{0} \\ \mathbf{B}_1 \mathbf{D}_1 + \mathbf{B}_2 \mathbf{C}_2 & \mathbf{A}_1 & \mathbf{B}_2 \mathbf{C}_3 \\ \mathbf{0} & \mathbf{0} & -\mathbf{L}^{-1} \mathbf{R} \end{bmatrix} \begin{bmatrix} x_1 \\ z \\ i \end{bmatrix} + \begin{bmatrix} \mathbf{0} \\ \mathbf{0} \\ \mathbf{L}^{-1} \end{bmatrix} e \quad (27)$$

$$y = \begin{bmatrix} \mathbf{C}_1 & \mathbf{0} & \mathbf{0} \end{bmatrix} \begin{bmatrix} x_1 \\ z \\ i \end{bmatrix} \quad (28)$$

Where the parameters are given by,

$$x_1 = [x_s \quad y_s \quad z_s \quad \theta \quad \varphi]^T \quad (29)$$

$$z = x_1 \quad (30)$$

$$i = [i'_1 \quad i'_2 \quad i'_3 \quad i'_4]^T \quad (31)$$

$$e = [e'_1 \quad e'_2 \quad e'_3 \quad e'_4]^T \quad (32)$$

$$\mathbf{A}_1 = \begin{bmatrix} 0 & 0 & 0 & 0 & 0 \\ 0 & 0 & 0 & 0 & 0 \\ 0 & 0 & 0 & 0 & 0 \\ 0 & 0 & 0 & 0 & -p J_x / J_y \\ 0 & 0 & 0 & p J_x / J_y & 0 \end{bmatrix} \quad (33)$$

$$\mathbf{B}_1 = \begin{bmatrix} -1/m & -1/m & 0 & 0 & 0 & 0 \\ 0 & 0 & 1/m & 1/m & 0 & 0 \\ 0 & 0 & 0 & 0 & -1/m & -1/m \\ 0 & 0 & 0 & 0 & L_{01}/J_y & -L_{02}/J_y \\ 0 & 0 & L_{01}/J_y & -L_{02}/J_y & 0 & 0 \end{bmatrix} \quad (34)$$

$$\mathbf{B}_2 = \begin{bmatrix} 1/m & 1/m & 1/m & 1/m \\ 0 & 0 & 0 & 0 \\ 0 & 0 & 0 & 0 \\ -1/J_y & 0 & 1/J_y & 0 \\ 0 & -1/J_y & 0 & 1/J_y \end{bmatrix} \quad (35)$$

$$\mathbf{C}_1 = \begin{bmatrix} 1 & 0 & 0 & -i' & 0 \\ 1 & 0 & 0 & 0 & -i' \\ 1 & 0 & 0 & i' & 0 \\ 1 & 0 & 0 & 0 & i' \end{bmatrix} \quad (36)$$

$$\mathbf{C}_2 = \begin{bmatrix} 2F_1/W & 0 & 0 & -2lF_1/W & 0 \\ 2F_2/W & 0 & 0 & 0 & -2lF_2/W \\ 2F_3/W & 0 & 0 & 2lF_3/W & 0 \\ 2F_4/W & 0 & 0 & 0 & 2lF_4/W \end{bmatrix} \quad (37)$$

$$\mathbf{C}_3 = \text{diag} [2F_1/I_1 \quad 2F_2/I_2 \quad 2F_3/I_3 \quad 2F_4/I_4] \quad (38)$$

$$\mathbf{D}_1 = \begin{bmatrix} -S_b & 0 & -T_l & T_l L_{01} & 0 \\ -S_r & 0 & -T_r & -T_r L_{02} & 0 \\ 0 & -R_y & 0 & 0 & -R_b L_{01} \\ 0 & -R_{ry} & 0 & 0 & R_r L_{02} \\ -U_l & 0 & Q_{lc} & -Q_{lc} L_{01} & 0 \\ -U_r & 0 & Q_{rc} & Q_{rc} L_{02} & 0 \end{bmatrix} \quad (39)$$

$$T = \partial f_s / \partial z \text{ at } z_0$$

$$U = \partial f_c / \partial x \text{ at } x_0$$

$$\mathbf{R} = \text{diag} [R_1 \quad R_2 \quad R_3 \quad R_4] \quad (40)$$

$$\mathbf{L} = \text{diag} [L_1 \quad L_2 \quad L_3 \quad L_4] \quad (41)$$

The above equations in Eqs.(27) and (28) are the detailed modeling for controlling pitch, yaw and axial displacement. Firstly we have taken a simplified scheme. In the simplified approach, signal from only one gap sensor have been used and all the electromagnets are connected in series, the system equations reduced to as shown in Eqs.(42) and (43).

$$\frac{d}{dt} \begin{bmatrix} x' \\ \dot{x}' \\ i' \end{bmatrix} = \begin{bmatrix} 0 & 1 & 0 \\ \frac{2S}{m} + \frac{2}{mW} \sum_i F_i & 0 & \frac{2}{ml} \sum F_i \\ 0 & 0 & -\frac{l}{L} \end{bmatrix} \begin{bmatrix} x' \\ \dot{x}' \\ i' \end{bmatrix} + \begin{bmatrix} 0 \\ 0 \\ \frac{1}{L} \end{bmatrix} e' \quad (42)$$

$$y = [1 \quad 0 \quad 0] \begin{bmatrix} x' \\ \dot{x}' \\ i' \end{bmatrix} \quad (43)$$

The parameters used in this model are explained below

- x' : Gap derivation from nominal state
- i' : Current derivation of electromagnet from nominal state
- e' : Incremental input voltage to electromagnet
- m : Mass of rotor
- F_i : Attractive force at steady state
- I : Nominal current
- W : Nominal gap
- r : Resistance of electromagnet
- L : Inductance of electromagnet
- S : Constant used in permanent magnet equation

6. Solution to Control Problem

Using equations Eqs.(42) and (43) for the stability of the system which is unstable in nature, an optimum integral type servo control system has been constructed. Using this control system the experiment on the model has been carried out. By using MATLAB, the Riccati equations are solved to obtain the feedback coefficients for stabilization of the unstable system. An interactive program has been developed with the DSP which takes four gain parameters from keyboard and sends to the target program and the DAC output is represented as

$$e' = - \left(k_1 x' + k_2 \frac{dx'}{dt} + k_3 i' + k_4 \int x' dt \right) \quad (44)$$

The parameters used for the solutions are listed in Tables 1 to 3. The system has been simulated with help of MATLAB. Fig.11 shows the simulated response characteristics of the system.

Table 1 Parameters of electromagnet.

Parameter	Symbol	Value	Unit
Resistance	r	11.72	Ω
Inductance	L	0.194	H
Steady current	I	1.0	A
Steady attractive force	F ₁₋₄	5.88	N

Table 2 Rotor parameters.

Parameter	Symbol	Value	Unit
Mass of rotor	m	8.0	kg
Moment of inertia	J _x	2.379 × 10 ²	kg · m ²
	J _y	8.364 × 10 ²	kg · m ²
Radius of fly-wheel	r _s	1.15 × 10 ¹	m
Length of shaft	L _e	5.1 × 10 ¹	m
Length between rotor magnet and fly-wheel	L ₀₁	1.65 × 10 ¹	m
	L ₀₂	1.65 × 10 ¹	m

Table 3 Parameters of permanent magnet.

Parameter	Symbol	Value	Unit
Steady repulsive force	F _a	39.2	N
	F _b	0	N
	F _c	11.76	N
Stiffness	Q _e	4.90 × 10 ³	N/m
	R _b	2.52 × 10 ³	N/m
	S _e	1.18 × 10 ⁴	N/m
	T _p , T _r	-3.12 × 10 ²	N/m
	U _p , U _r	-4.90 × 10 ²	N/m

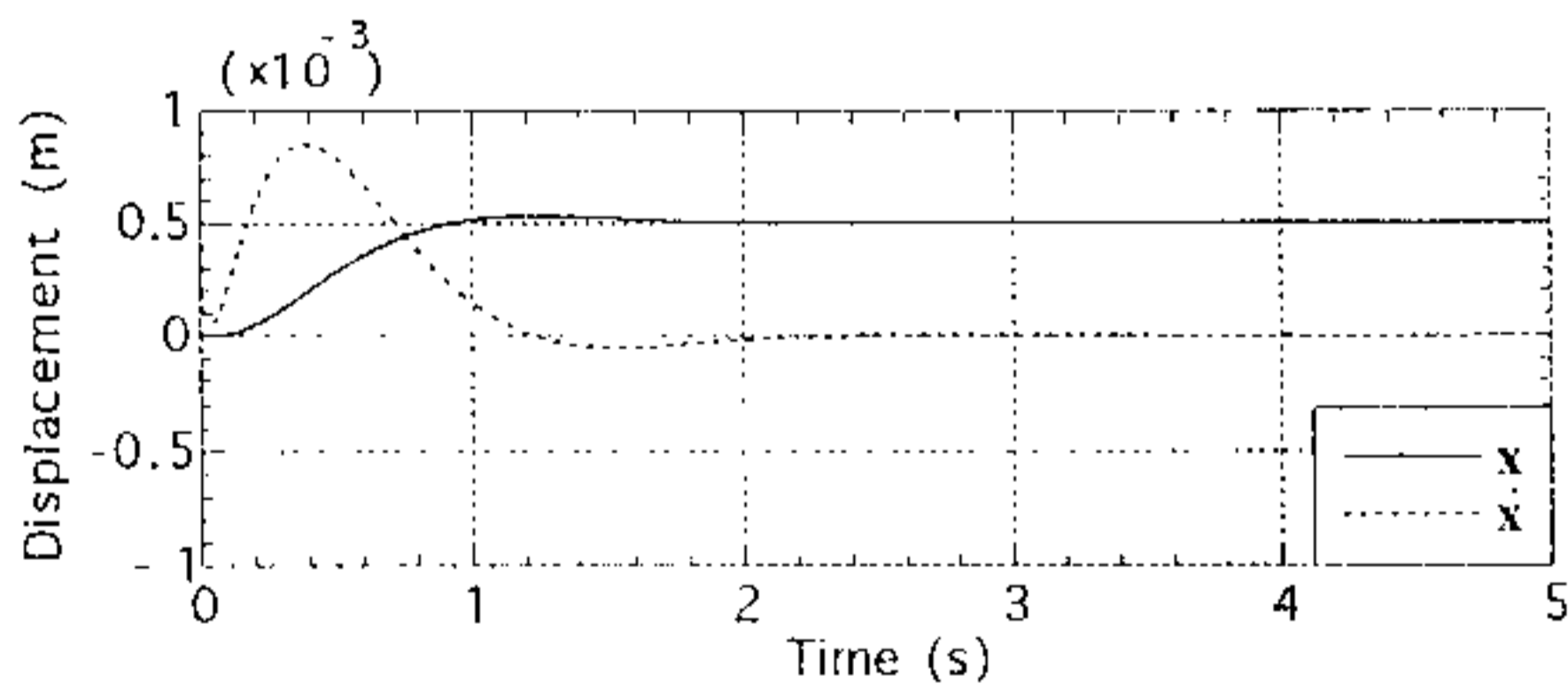


Fig. 11 Simulated vibration characteristics of rotor.

7. Experimental Results

The experiments are carried out by configuring the controller around the digital signal processor. The block diagram representation of the control system is shown in Fig.12. The inputs to the controller are the gap displacement, its derivative and the current of the electromagnet.

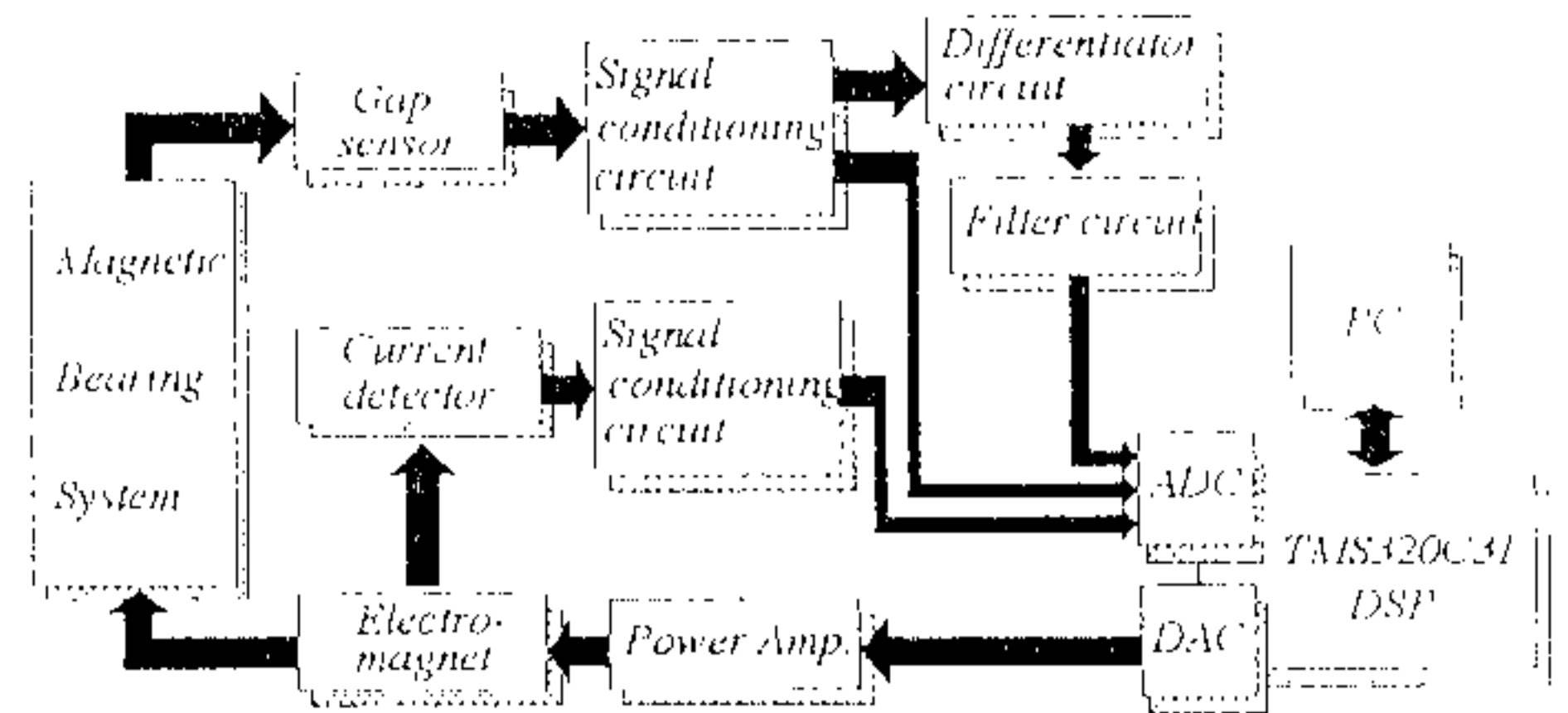


Fig. 12 Controller block diagram.

Using the above controller the experiments has been conducted and the rotor of the motor has been stabilized. The vibration of the rotor along x-axis is within 10 micrometer at steady state. When disturbance is created the system shows overshoot and comes back to original condition fast represents the controller is robust in nature. Figs. 14(a) and 14(b) show the vibration characteristics at turn-on and turn-off disturbance respectively. In this case a disturbance step function 0.5 mm has been created not by physically applying force on the rotor but by adding it to the feedback signal for the gap sensor. The system takes approximately 1.0 sec. to drive away out all the transients and returns to steady state. As the disturbance is created along x-axis, the rotor does not shift along z-axis and y-axis at steady state which has been confirmed by experiment.

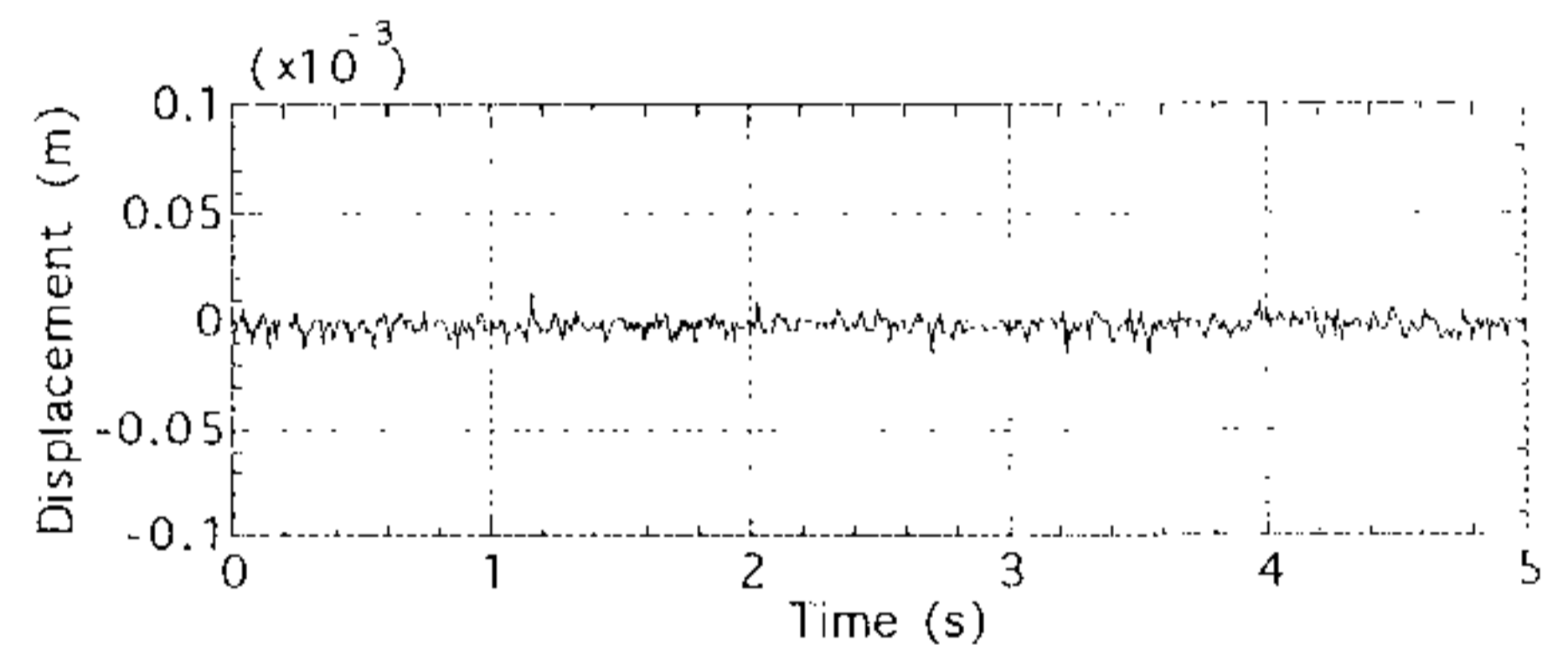
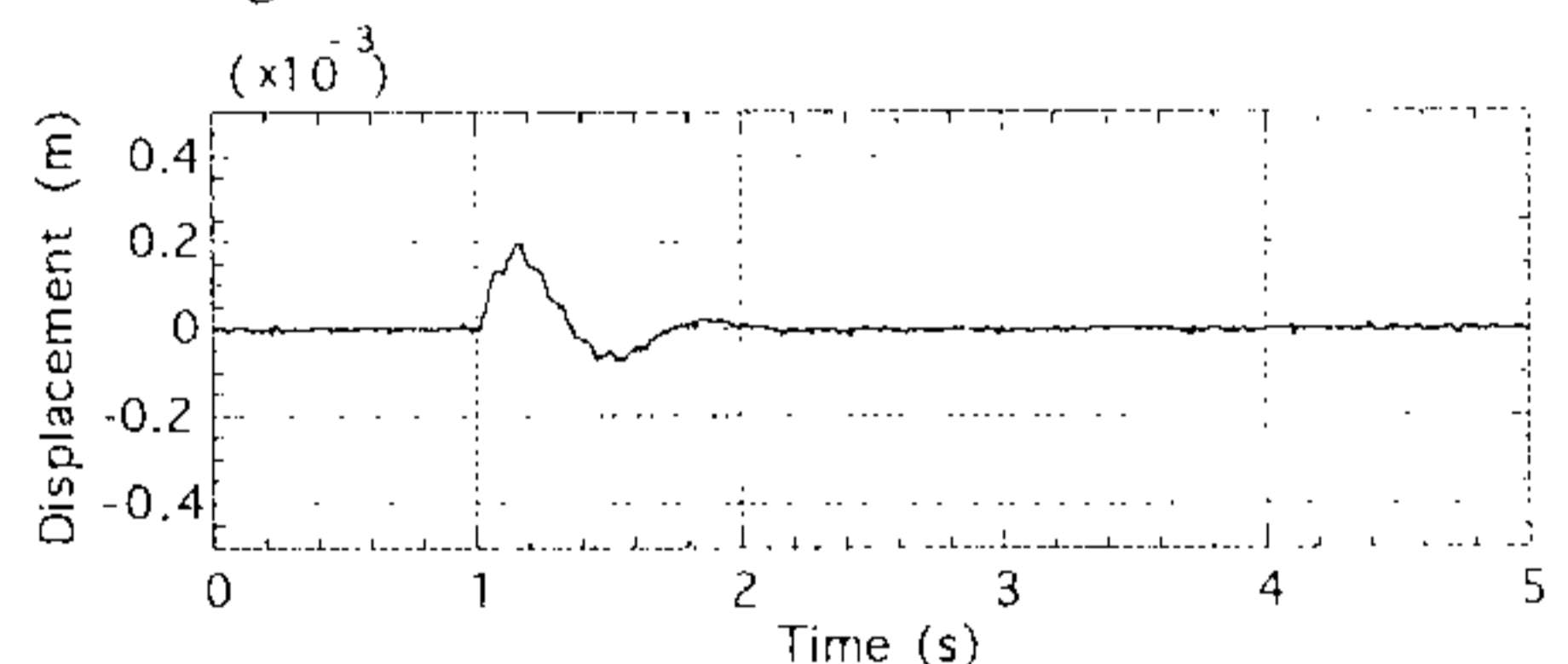
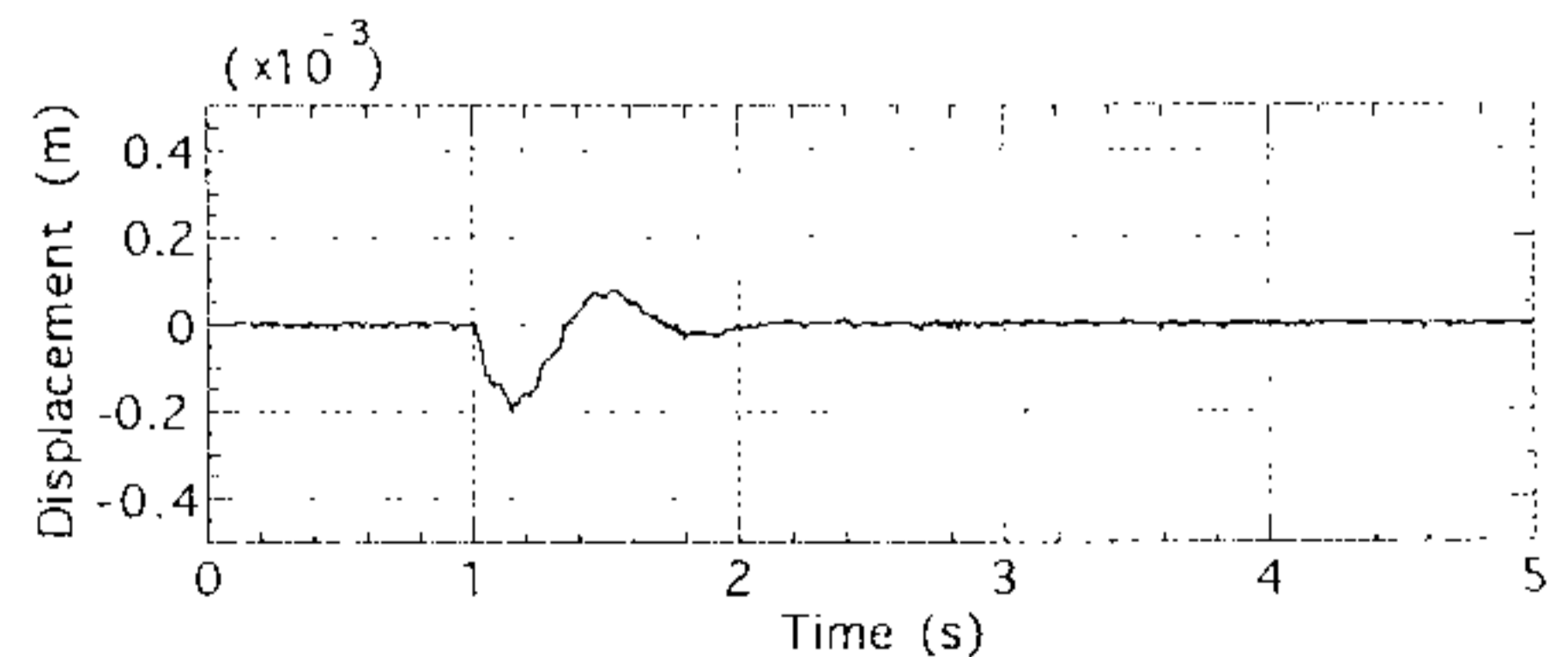


Fig. 13 Vibration characteristic of rotor.



(a) Turn-on disturbance



(b) Turn-off disturbance

Fig. 14 Disturbance characteristics.

8. Conclusions

This paper has described the development of a new repulsive type magnetic bearing system using permanent magnets for the levitation and radial control. Axial controls have been achieved by controlled electromagnets. The system equations are discussed and the modeling of the real physical repulsive type magnetic bearing system have been formulated. By constructing an integral type servo control system and configuring the controller around the digital signal processor the rotor shaft has been stabilized in the desired position. The experimental results are also very much satisfactory which promises low cost alternative of using this type of magnetic bearing systems in industrial applications.

References

- [1] Jean-Paul Yonnet, "Passive Magnetic Bearing with Permanent Magnets", IEEE Trans. on Magnetics, Vol-MAG 14, No. 5, pp.803-805, Sept. 1978.
- [2] Jean-Paul Yonnet, "Permanent Magnet Bearings and Couplings", IEEE Trans. on Magnetics, Vol-MAG 17, No. 1, pp.1169-1173, Jan. 1981.
- [3] J.P. Yonnet, S.Hemmerlin, E.Rulliere and G.LEmarquand, "Analytical Calculation of Permanent Magnet Couplings", IEEE Trans. on Magnetics, Vol-MAG 29, No. 6, pp. 2932-2934, Nov. 1993.
- [4] J. Delamare, E.Rulliere and J.P.Yonnet, "Classification and Synthesis of Permanent Magnet Bearing Configuration", IEEE Trans. on Magnetics, Vol-MAG 31, No. 6, pp.4190-4192, Nov. 1995.
- [5] Magnetic Levitation and Magnetic Control, Chap-5, Corona Co, 1993(in Japanese).
- [6] T. Ohji, T.Miyamoto, S.Yamada and F.Matsumura, "Single-Axis Controlled Repulsion Type Magnetic Bearing System Using Permanent Magnets", Proceeding of 7th National Conference on Electromagnetics and Dynamics, pp.189-194, 1995 (in Japanese).
- [7] F.Matsumura and H.Kobayashi, "Fundamental Equation for Horizontal Shaft Magnetic Bearing and Its Control System Design", Journal of Electrical Engineering in Japan, Vol. 101C, No. 6, pp.137-144, June 1981 (in Japanese).
- [8] F.Matsumura and T.Yoshimoto, "System Modeling and Control design of a Horizontal-shaft Magnetic Bearing System", IEEE Trans. on Magnetics, Vol. MAG-22, No. 3, pp.196-203, May 1986.